Int. J. Heat Mass Transfer. Vol. 22, pp. 421–430

0017-9310/79/0301-0421 $02.00/0

NATURAL CONVECTION IN A VERTICAL CYLINDER SUBJECT TO CONSTANT HEAT FLUX

C. F. HESS and C. W. MILLER†
Department of Mechanical Engineering, University of California, Berkeley, CA 94720, U.S.A.

Abstract—An experimental investigation was done using a laser Doppler velocimeter to measure the axial velocity of a fluid contained in a cylinder subject to constant heat flux on the side walls. Velocities as low as 0.025 cm/s could be resolved. The error for typical velocities in the boundary layer is ± 10%. The modified Rayleigh numbers studied ranged between 4.5×10^9 and 6.4×10^{10}, which correspond to the upper limit of the laminar regime. The flow field inside the boundary layer was divided into three regions along the axis of the cylinder and a parabolic distribution was used to fit the data within each region. Excellent agreement was found with an available numerical solution.

NOMENCLATURE

- d, diameter of laser beam before going through lens;
- D, internal diameter of cylindrical enclosure;
- dl, diameter of laser beam at the waist;
- dm, dimension of probe volume in axial direction;
- F, focal length of focusing lens;
- f_D, Doppler frequency;
- g, acceleration of gravity;
- h, axial coordinate ($h = 0$ at bottom of cylinder);
- h_1, height that defines Region I;
- h_2, height that defines Region II;
- K, constant in equation (5);
- k, thermal conductivity;
- L, total height of cylinder;
- lm, dimension of probe volume in radial direction;
- Pr, Prandtl number $= \nu/\alpha$;
- q_w, heat flux at the side walls of cylinder;
- R, radial coordinate ($R = 0$ at the wall);
- Ro, total radius of cylinder ($D/2$);
- Ra_L^*, modified Rayleigh number $= \dfrac{g\beta q_w L^4}{k\nu\alpha}$;
- T, temperature;
- U, axial velocity;
- W, constant in equations (6), (7) and (8).

Greek symbols

- α, thermal diffusivity;
- β, coefficient of volumetric expansion;
- δ_0, boundary-layer thickness defined at $U = 0$;
- δ_1, boundary-layer thickness defined at maximum velocity;
- λ, wavelength of laser beam;
- θ, angle between two laser beams in air;
- ν, kinematic viscosity.

†Present address: Earth Sciences Division, Lawrence Berkeley Laboratory, Berkeley, CA 94720, U.S.A.

INTRODUCTION

NATURAL convection in fluids contained in an enclosure is encountered in many engineering applications, including the storage of cryogenic fluids, petroleum storage vessels on hot days, the thermal response of a building to a change in environment temperature, and the storage of hot fluids for solar power plants. In all these cases, the heat loss from or to the enclosure is an important problem. Extensive analytical and experimental work has been conducted with fluids in an enclosure subject to different boundary conditions, but the specific problem that will be considered here is that of constant heat influx at the side walls of a filled cylindrical container. The case of a partially filled container has been analyzed previously both theoretically and experimentally, but even in this case, no experimental verification of the detailed velocity profiles has been provided which could substantiate any of the theories postulated. The previous experimental studies provided gross ideas of the flow behavior because the methods used only measured an average effect of the velocity. The measurements reported here give detailed axial velocities as a function of time and position.

In 1966, Clark [1] reviewed the literature on the work that had been done on fluids enclosed in vessels subject to constant heat flux on the side walls and its effect on the stratification of the fluid. Schwind and Vliet [2] studied free convection in vessels subject to constant heat flux using schlieren and shadowgraph methods. They were not able to provide any details of the velocity profiles nor the magnitude of the velocity inside the boundary layer. They were able only to obtain a qualitative sketch of the boundary-layer thickness once the flow was quasi-steady. Neff and Chiang [3] also did experiments in an enclosure uniformly heated; they used hollow glass microspheres of neutral density to illustrate the flow field. Evans *et al.* [4] did some temperature measurements and dye tracing. They also presented a simplified model using the integral forms of the momentum and energy equations. This model seems to provide good results for the

temperature behavior but no experimental values of the velocity are available for comparison. The subdivision of the flow field was similar to the one suggested by Clark [1], namely a three region model. The main core grows with a plug velocity U_c which seems to be a reasonable assumption for high Rayleigh numbers. Fan, Chu and Scott [5] did experimental and theoretical work on temperature profiles in pressurized cryogenic vessels subject to a time dependent uniform heat flux. Their theoretical work ignores the axial velocity to obtain linear uncoupled equations that enables them to use Duhamel's theory of superposition. This is a gross oversimplification of the problem since convection is the main mechanism in creating stratification. Other relevant experimental studies are by Huntley [6], Harper *et al.* [7], Evans and Stefany [8]. Barakat and Clark [9] presented a numerical solution to the two-dimensional, laminar, transient free convection in a partially filled liquid container subject to an arbitrary wall temperature. Results of the temperature and streamline profiles were presented as well as some experimental data for the temperature. But their reported results were limited to lower Rayleigh numbers. Miller [10] used a finite difference scheme with variable grid size to solve the flow field and temperature profiles of a fluid in an enclosure subject to constant heat flux on the side walls and insulated on the top and bottom. The numerical technique utilized to solve this problem was presented in [11] where the more general problem, a stratified flow subject to an arbitrary transient wall temperature, is solved. Jischke and Doty [12] solved a simplified version of the problem by obtaining solutions to the linearized form of the Boussinesq equations using a modified asymptotic expansion analysis. Some basic ideas and the problems to solve the flow in enclosures are presented in a review paper by Ostrach [13].

It is the purpose of this paper to provide some experimental results, both in the transient and quasi-steady regime, on the axial velocity in a fluid contained in an enclosure subject to a constant heat flux. These results are compared to the numerical studies of Miller [10] and Evans, Reid and Drake [4]. The techniques available until recently: dye tracing,† high speed photography, schlieren methods, etc. did not permit detailed solutions to free convection flows because they could not measure instantaneous velocities or densities at a given location; they do provide, however, a general gross behavior of the stream lines and permit the development of simple models. A laser-Doppler velocimeter (LDV) was used in the experiments presented in this paper. It measures, accurately and without disturbing the flow, instantaneous velocities at a probe volume the size of which is adjusted by the choice of optics.

†The axisymmetry of the velocity field was checked by dye tracing prior to the use of LDV.

With this LDV system, velocities of 0.025 cm/s can be resolved with an accuracy of $\pm 20\%$. For the typical velocities in the boundary layer (0.25 cm/s) the accuracy is about $\pm 10\%$. The time response is very small, on the order of 10^{-8} s. The tracker was processing about 1000 samples/s, hence, instantaneous changes in the velocity could easily be followed. A comprehensive study of laser-Doppler technology can be obtained in [14] and [15].

EXPERIMENTAL SYSTEM

Apparatus

The experimental apparatus consisted of both a cylindrical tank as the enclosure and a laser-Doppler velocimeter (LDV) used to measure the fluid velocity. The tank, as shown in Fig. 1, had an I.D. of 24 cm, and O.D. of 25.4 cm, a height of 38 cm, and

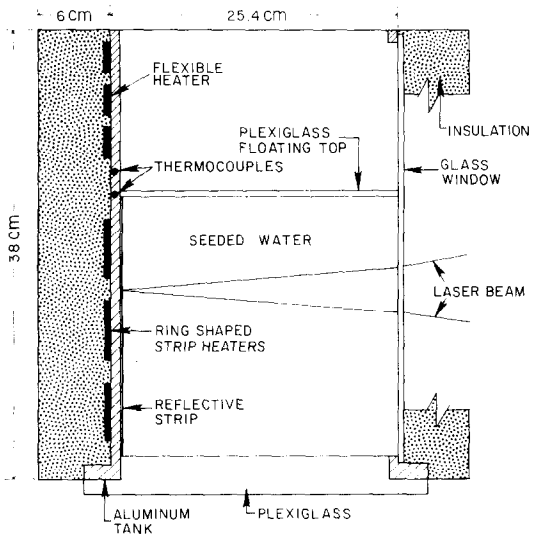

FIG. 1. Cylindrical enclosure.

was made of aluminum 6061-T6. The constant heat flux was provided by three strip heaters (maximum output was 750 W each) shaped as a ring to fit on the tank, with an opening of 5 cm to allow space for a window. Since only a portion of the tank was filled with fluid, a flexible guard heater (output 750 W) was used at the top of the enclosure at the wall to prevent heat loss up the side of the tank. Two copper–constantan thermocouples were placed in the wall of the tank between the water level and the guard heater set above the water level. The voltage to the guard heater was adjusted until both thermocouples read the same value, implying no heat loss in the axial direction. For both the heaters and the guard heater, variable voltage sources were used. In addition, the entire system, except needed windows, was insulated with fiberglass and porous rubber.

To permit transmission of the laser beam and collection of the scattered light, windows in the enclosure were necessary. Because only the effect of the side wall was being investigated, clear Plexiglas, 3.2 cm thick, was used both for the top and bottom

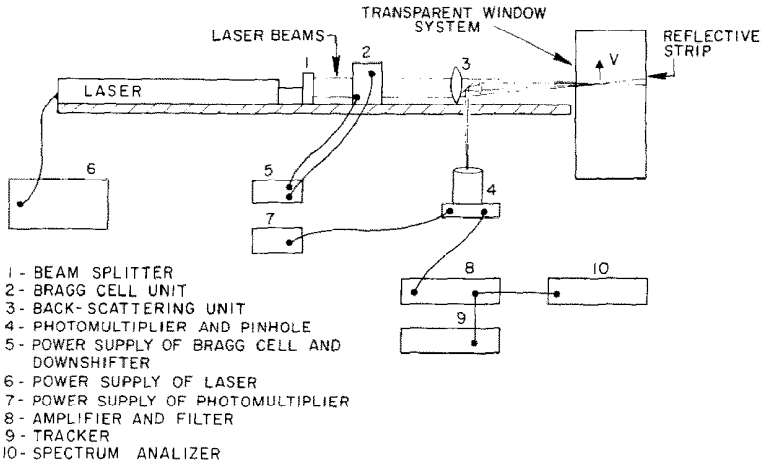

FIG. 2. Schematic representation of laser-Doppler velocimeter.

of the enclosure. Besides being transparent, the Plexiglas provided insulation. The bottom was attached to a flange and was flush to the side wall. The top was machined so it could float on water. In this way, the aspect ratio could be changed easily. One disadvantage of using the floating top was that the aspect ratio changed slightly due to the expansion of the water as it heated up. A maximum change of 0.2% was observed in 1 h for the conditions of these experiments. Although this is small, it had to be compensated for when determining the position of the probe volume near the top.

To measure the axial velocity component, a glass window 2.54 cm wide and 0.5 cm thick was placed on the side of the tank extending from the top to the bottom. This window introduced an error on the axial symmetry of the fluid velocity. However, to reduce this error the velocity measurements were made across the tank from the window.

Laser-Doppler velocimeter

As stated, a laser-Doppler velocimeter (LDV) was used to measure the small velocities characteristic of natural convection. In the LDV system, a laser beam is split into two beams and focused at the desired point of measurement. The size of the probe volume is given by:

$$dm = \frac{dl}{\cos(\theta/2)}, \tag{1}$$

$$lm = \frac{dl}{\sin(\theta/2)}, \tag{2}$$

where

$$dl = 3.183\lambda F/d_{1/e^2}. \tag{3}$$

For the conditions of the experiment $dm = 0.27$ mm and $lm = 2.7$ mm. A particle passing through this probe volume will scatter light with a time variation that contains the information of its velocity. The velocity of the particle is then related to the wavelength λ of the laser, the frequency f_D of the scattered light and the optical set up by the following equation:

$$U = \frac{f_D\lambda}{2\sin(\theta/2)}. \tag{4}$$

The LDV measuring equipment is illustrated in Fig. 2. For this experiment, the 0.5146 μm line from a 2W MTM argon ion (Lexel, Model 85) was used.

Because the Doppler frequencies that correspond to the natural convection velocities are on the order of 500 Hz, which is below the range of available frequency trackers, a frequency shift system was needed. The shift had to be accurate to at least ±20 Hz. An acoustooptic (Bragg) cell (TSI Model 980) was used because of its long-term stability and accuracy (±10 Hz). A TSI model 915 compensated beam splitter split the laser beam into two equal intensity and coherent beams. One of the two beams was shifted optically by 40 MHz before it was focused on the probe volume. The light scattered from the probe volume had a frequency of $f_d + 40$ MHz. After passing through a set of pinholes, the scattered light was focused on the photomultiplier tube which output an electric signal with the same time dependence. This signal was amplified in a Keithley 107 pulse amplifier, filtered in a 42 MHz low pass filter and electronically downshifted to $f_D + 10$ kHz on a TSI Model 985. This output was filtered on a Krohn-Hite band pass filter (6 to 15 kHz) to eliminate low frequency noise and the harmonics generated by the TSI downshifter. The signal was processed in a TSI 1090 tracker with an added low range of 0.2 to 50 kHz.

Some special techniques were necessary in order to resolve the flow near the top and to optimize the signal-to-noise ratio. Two mirrors, made of low expansion substrates flat to 1/10 wave, were used to deflect the beams before they hit the lens in such a way that the beam closer to the top wall was parallel to it when coming out of the lens, and the second beam formed an angle of 12.8° at the intersection, allowing measurements to be made right at the top.

However, this results in a quasi-axial velocity, 6.4° from the vertical.

A very thin (0.0051 cm) reflective film, Scotch Tape No. 850, was placed opposite to the glass window to reflect the forward scattering from the probe volume formed by a dual beam mode. Backscattering was also possible but the reflection from the forward scattering was two orders of magnitude larger than the backscattering. The tank was rotated 7° and the transmitting optics were horizontally translated until the beams entered the glass window through the center. The reflection of the probe volume was expanded with this tilted mirror technique and the spatial resolution was increased permitting measurements at 0.06 cm from the wall. There was an error involved in this technique because the overall heat resistance was increased by 10% locally along the wall. However, this error was attenuated because the flow field in an enclosure depends on the overall heat transfer. The tank was black anodized to minimize multiple reflections that would increase the noise level. The laser, transmitting optics and receiving optics were secured to a rigid table made of 2.5 cm aluminum and 2.5 cm compressed wood attached to a three direction transverse mechanism. The enclosure was not moved during an experiment.

Experimental procedure

Two types of experiments were performed, one designed to measure the velocity profiles after an extended period of time as a function of the coordinate system and the other to measure the transient behavior very close to the top wall, which some authors refer to as the mixing region. Either experiment started by setting the temperature of the water and the walls of the tank to the initial conditions. This was done in two steps. The water was heated to $T_i = 25°C$ (very close to ambient) in a separate insulated container, using a Haake E-52 temperature controller assembly which is accurate to 0.1 K. The walls were heated to the same temperature using the heaters and the guard heater. The water was seeded and poured into the cylinder which was then covered with the floating top. Plastic pigments (Dow Chemicals No. 722) were used to seed the water. They are neutrally buoyant and provide enough scattering (signal-to-noise = 15) when using the reflective film technique. The system was allowed to rest (15 min) until no evidence of the initial motion could be observed with the LDV. For the quasi-steady experiments the heaters and guard heater were turned on at a time set equal to zero, and the transient velocity at a selected position was recorded to estimate the time required to reach quasi-steady. This time is a function of the heat input and the position. Longer times correspond to a low heat input and for positions close to the bottom of the tank. For the Ra_L^* used in this experiment, the time before quasi-steady was typically 15–20 min. Data was taken after 30 min to ensure that the quasi-steady state was reached. The probe volume was zeroed in reference to the upper or lower wall, and it was intersected on the wall opposite to the glass window (on the reflective film). The probe volume was then set at a given height and its radial position was varied. The velocity was measured at each position. It was double checked at the end of each experiment, which lasted about 30 min, to make sure of the existence of a quasi-steady state regime. To measure velocities outside the boundary layer the tilted mirror technique proved to be inconvenient because the image of the probe volume was distorted (which does not affect the signal), and it was difficult to align. The tank was not rotated for those points because outside the boundary layer there is a high spatial resolution. After each experiment the tank was cooled down and then set to the initial temperature (25°C).

Three different heat fluxes were used: 50 W/m^2, 250 W/m^2, and 600 W/m^2. For each heat flux condition, the velocity was measured at 13 axial positions providing a very complete picture of the flow field.

The transient experiments followed the same referencing technique, except that in these experiments the probe volume was set to a given position and not moved. The velocity of this position was recorded as a function of time, usually for 15 min, and the new experiment was started at a different position. Because of the variation of the index of refraction with temperature, the probe volume will move. However, very small temperature changes were imposed on the water, 5 K, which correspond to the maximum heat input of 600 W/m^2. The probe volume moves towards the center 0.001 cm/K for a change from 25 to 30°C.

RESULTS AND DISCUSSION

Experimental measurements of the axial velocity were made for 13 axial positions, 16 radial positions, four different times and four different heat inputs. The most relevant data is presented here. It was found that after a short time, the flow approached a quasi-steady state as has been observed previously [2]. The velocity does not continue growing as is the case for constant heat input to a vertical flat plate, because of the drag induced by the recirculation zone. Measurements were taken in both the transient regime and the quasi-steady. The axial velocity profile that exists in each of these regimes will be discussed separately.

Quasi-steady regime

Representative profiles of the experimentally measured axial velocity component for $Ra_L^* = 2.5 \times 10^{10}$ are shown in Figs. 3 and 4 for six different heights. The velocity profiles for a closed cylinder are close in appearance to the velocity profiles between two finite vertical plates; i.e. the axial velocity starts at zero at the wall and rapidly grows to its maximum value which defines the thickness of the boundary layer δ_1, it slowly goes to zero (at δ_0), and then changes

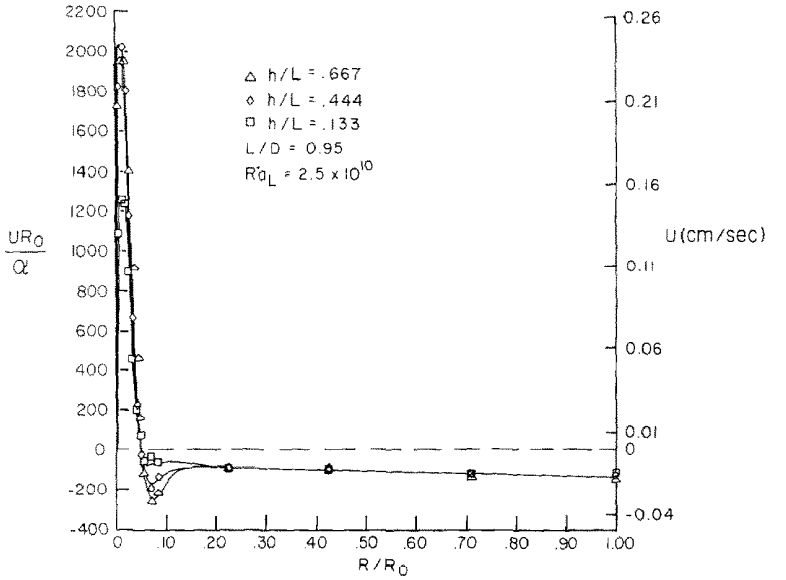

FIG. 3. Variation of axial velocity with radius ($R/Ro = 0$ at the wall, $h/L = 0$ at the bottom) for three different heights, in the bottom part of the cylinder, $q_w = 250\ \mathrm{W/m^2}$.

direction indicating the presence of a recirculating zone. This recirculating zone is more pronounced right after δ_0, then the velocity becomes almost constant all the way to the center of the tank. Since the flow is axisymmetric, only half of the cylinder is shown. Both δ_1 and δ_0 appear to be constant with only the velocity varying as a function of time. Because this is a closed cylinder, the axial velocity is zero at the bottom and top. A typical velocity profile inside the boundary layer as a function of height is shown in Fig. 5 for a constant radius and three different heat inputs. Note that $h/L = 0$ corresponds to the bottom of the tank while $R/Ro = 0$ is at the wall. From Figs. 3, 4 and 5 one can see that the flow field near the wall can be further divided into three regions, one very close to the bottom, the other very close to the top and a very large one halfway up the tank ($h/L = 0.5$). A discussion of the three regions follows.

Region I. This region ($h \leqslant h_1$) close to the bottom of the tank is characterized by a velocity profile which behaves similarly to the one generated by a vertical flat plate with constant heat input. Some differences exist since the recirculating zone will cover the tank through its total height after an extended period of time. A modified solution to the integral form of the equations of energy and momentum as obtained by Evans [4] yields the following expression for the velocity profile:

$$U(h, r) = K\left(\frac{h}{L}\right)^{3/5}\left(\frac{R}{\delta_0}\right)\left(1 - \frac{R}{\delta_0}\right)^2 \qquad (5)$$

for $r \leqslant \delta_0$. Table 1 contains the limiting values of δ_0 and δ_1 for the end of Region I. These values, which

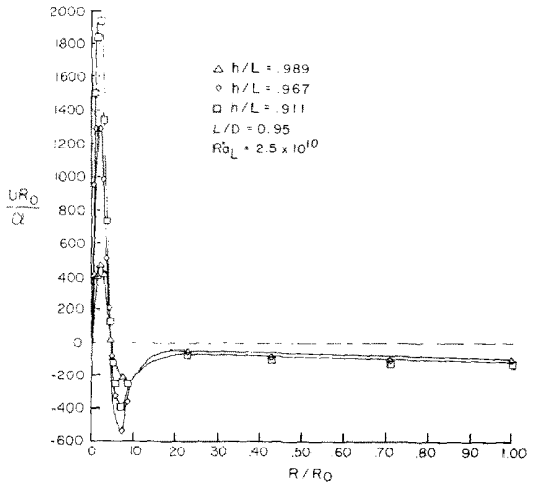

FIG. 4. Variation of axial velocity with radius ($R/Ro = 0$ at the wall, $h/L = 0$ at the bottom) for three different heights near the top, $q_w = 250\ \mathrm{W/m^2}$.

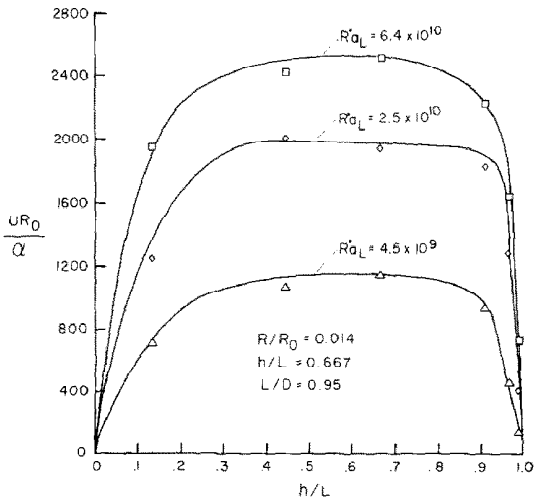

FIG. 5. Variation of axial velocity with height ($h/L = 0$ at the bottom) $q_w = 50\ \mathrm{W/m^2}$, $250\ \mathrm{W/m^2}$ and $600\ \mathrm{W/m^2}$.

Table 1.

Ra_L^*	K (cm/s)	$\frac{\delta_0}{Ro}$ (experimental)	$\frac{\delta_1}{Ro}$ (experimental)	$\frac{\delta_1}{Ro}$ [10]	$\frac{\delta_1}{Ro}$ [10]
4.5×10^9	2.1	0.068	0.026	0.07	0.025
2.5×10^{10}	3.5	0.045	0.017		
6.4×10^{10}	5.5	0.036	0.013		

remain constant through Regions II and III, were used to fit equation (5) and provide K. The estimated value of δ_0 using flat plate analysis is 30% thinner than experimental results. The numerical results obtained by Miller [10] are in good agreement with experimental results. Figure 6 contains plots of the experimental results, equation (5) and Miller's [10] results. Evans [4] estimates the entire flow field inside the boundary layer using the flat plate analysis but does allow the bulk temperature to vary with time and position. This results in a boundary-layer thickness consistently thinner than

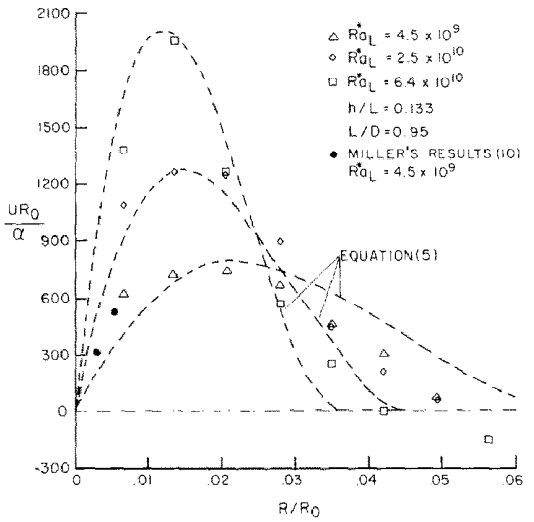

FIG. 6. Variation of axial velocity with radius ($R/Ro = 0$ at the wall) inside the boundary layer for three different heat inputs (50 W/m^2, 250 W/m^2, 600 W/m^2) in Region I. The experimental results were presented together with Miller's results [10] and equation (5).

experimental and numerical [10] results. Also the velocity profiles ignore the fact that the axial velocity is zero at the top giving rise to recirculation.

Region II. In this region ($h_1 < h < h_2$) the velocity is almost flat (independent of h) indicating the presence of the top and in turn the recirculation of the flow. The recirculation leads to a variable bulk temperature (increasing with h) that balances the buoyant and friction forces resulting in a closely similar velocity profile. The general effect of a variable bulk temperature was analyzed by Schwind [2] and Evans [4]. The boundary-layer thickness (δ_0, δ_1) in this region remains constant. The velocity profile can be approximated using the same analysis as in Region I by:

$$U(r) = W\left(\frac{R}{\delta_0}\right)\left(1 - \frac{R}{\delta_0}\right)^2 \tag{6}$$

for $h_1 < h < h_2$ (Table 2) where W is a function of Ra_L^* and has units of velocity. Table 2 contains values of W for 3 different heat inputs.

Table 2.

Ra_L^*	W(cm/s)	h_1	h_2
4.5×10^9	1.06	0.25	0.92
2.5×10^{10}	1.66	0.30	0.95
6.4×10^{10}	2.10	0.30	0.95

The values of W, which are an indication of the maximum velocity inside the boundary layer, are closely related to Ra_L^* by the expression:

$$\frac{W_a}{W_b} = \left[\frac{(Ra_L^*)_a}{(Ra_L^*)_b}\right]^{1/4} \tag{7}$$

within the limits of the experiment, where a and b correspond to two different cases. Figure 7 contains some comparisons of the experimental data with equation (6) and Miller's [10] results. Note the close agreement with the numerical results. The value of

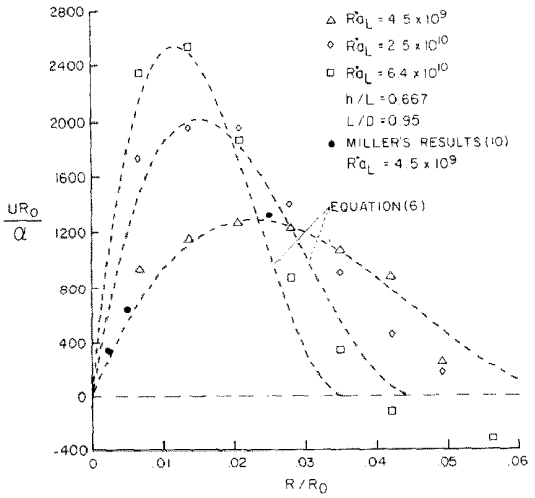

FIG. 7. Variation of axial velocity with radius ($R/Ro = 0$ at the wall) inside the boundary layer for three different heat inputs (50 W/m^2, 250 W/m^2, 600 W/m^2) in Region II. The experimental results are presented together with Miller's results [10] and equation (6).

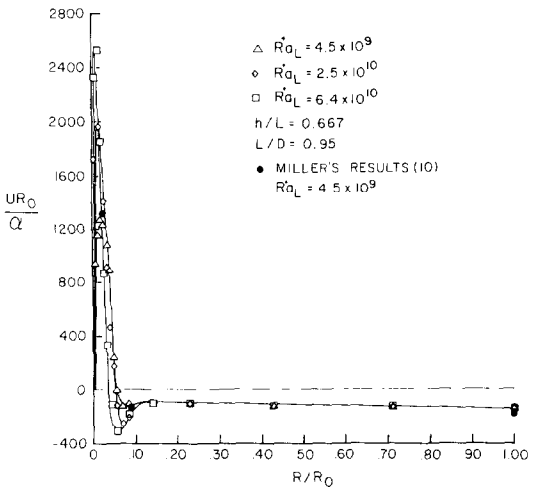

FIG. 8. Variation of axial velocity with radius ($R/Ro = 0$ at the wall) for the entire flow field in Region II. The experimental results are presented together with Miller's results [10].

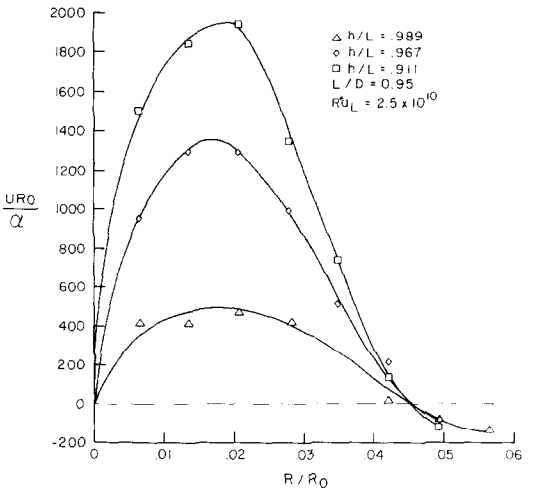

FIG. 9. Variation of axial velocity with radius ($R/Ro = 0$ at the wall, $h/L = 1$ at the top) inside the boundary layer for three different heights in Region III, $q_w = 250\ \mathrm{W/m^2}$.

the boundary-layer thickness used in equation (6) is the average for the whole region which is 20% thinner than for the specific location $h/L = 0.667$. The entire flow field for this region is shown in Fig. 8 for the three Rayleigh numbers and again the results obtained by Miller [10] are plotted for comparison.

Region III. This region ($h \geqslant h_2$) is characterized by a linear velocity profile in the axial direction indicating the presence of the boundary layer formed by the radial component of the velocity near the top. Clark [1] and Evans [4] refer to it as the mixing zone and estimate it using temperature measurements to be confined to the upper 10% of the vessel for a partially filled cylinder. Note from Table 2 that $h_2 = 0.92$ for $Ra_L^* = 4.5 \times 10^9$ which is of the same order as the estimation of Clark [1] and Evans [4]. This is not surprising since the partially filled cylinder has also the condition of zero axial velocity at the top. The value of h_2 increases with increasing Ra_L^* which results in a higher radial velocity and hence a thinner boundary layer. Figure 9 contains the experimental results of Region III for one Rayleigh number. The axial variation of the velocity is the same for different Ra_L^* with the maximum velocity and boundary layer varying as indicated in Fig. 10. The numerical results obtained by Miller [10] are also plotted in Fig. 10 demonstrating the agreement between the experiment and the finite difference scheme. The axial velocity in this region can be approximated by:

$$U(h,r) = \frac{W(L-h)}{(1-h_2)}\left(\frac{R}{\delta_0}\right)\left(1-\frac{R}{\delta_0}\right)^2 \qquad (8)$$

for $h \geqslant h_2$, which is an extension of equation (6) that satisfies the linear behavior of the velocity in the axial direction.

The velocity measurements made in 13 axial positions indicate a small variation of the boundary-layer thickness in Regions II and III (15% at the

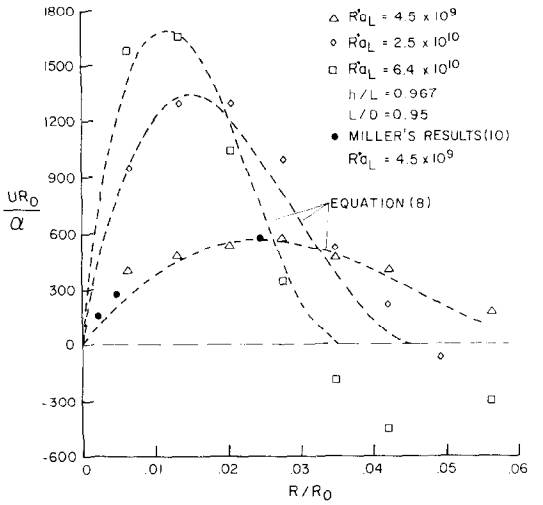

FIG. 10. Variation of axial velocity with radius ($R/Ro = 0$ at the wall) inside the boundary layer for three different heat inputs (50 W/m², 250 W/m², 600 W/m²) in Region III. The experimental results are presented together with Miller's results [10] and equation (8).

most). This constant boundary layer was also observed by Schwind and Vliet [2] and obtained numerically by Miller [10]. The variations of δ_1 and δ_0 with Ra_L^* are depicted in Fig. 11. A slope of $-1/4$ is obtained for both δ_0 and δ_1, that is:

$$\frac{\delta_a}{\delta_b} = \left[\frac{(Ra_L^*)_a}{(Ra_L^*)_b}\right]^{(-1/4)} \qquad (9)$$

where a and b correspond to two different cases. The same functional relationship is obtained for a vertical flat plate.

In general, there is a transition between zones and care must be taken when applying equations (5), (6) or (8). The values of h_1 and h_2 are functions of Ra_L^* and the aspect ratio L/D. More numerical calcu-

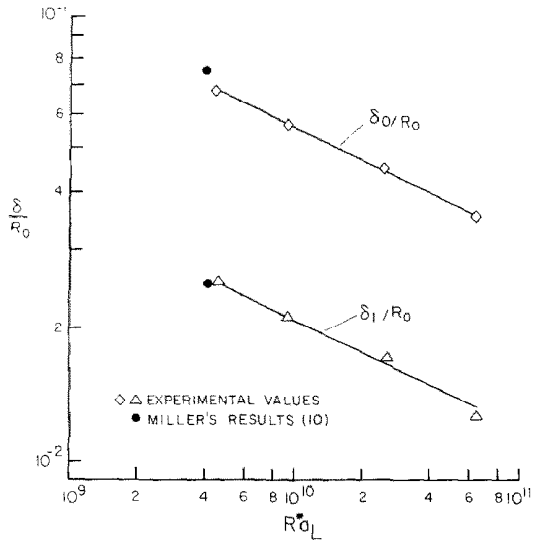

FIG. 11. Variation of δ_1 (radial position of maximum velocity) and δ_0 (radial position of zero velocity) with Rayleigh number.

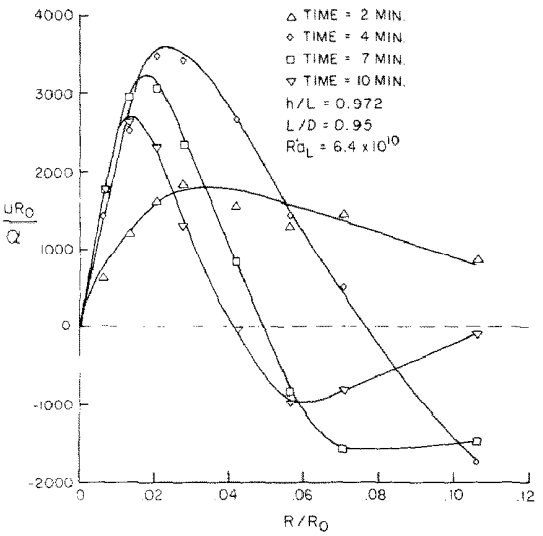

FIG. 12. Variation of axial velocity with radius ($R/Ro = 0$ at the wall) and time, $q_w = 600\ W/m^2$.

lations or experimental data would be necessary to obtain expressions for h_1 and h_2.

Outside the boundary layer there is a strong recirculation region of about the same width as the boundary-layer thickness, Figs. 3, 4 and 8. The velocity remains negative and almost constant from the strong recirculation region to the center of the tank. This partially confirms the assumptions of Clark [1] and Evans [4] who conceived a plug velocity outside the boundary layer.

The ascending flow rate (inside boundary layer) was computed by numerical integration of the velocity (assuming constant density) and compared to the returning flow outside the boundary layer at six axial positions and three Ra_L^*. The error was in the order of 10% for $Ra_L^* = 6.4 \times 10^{10}$, 13% for $Ra_L^* = 2.5 \times 10^{10}$ and 15% for $Ra_L^* = 4.5 \times 10^9$.

Transient regime

The velocity profiles are plotted as functions of radius and time in Fig. 12 for $h/L = 0.967$ and $Ra_L^* = 6.4 \times 10^{10}$. Note that the basic parabolic shape is obtained after a short period of time (about 4 min) and is maintained through the quasi-steady regime. It takes about 30 s to detect a measurable velocity at 0.1 cm from the wall. Part of this delay is due to the heat capacity of the tank and the exterior of the heaters. Inside the boundary layer the velocity starts growing as a function of time and reaches a maximum value at about 4 min. It then starts decaying approaching the quasi-steady regime (after 15 min). The rate change of the velocity decreases with time as it approaches quasi-steady.

The boundary-layer thickness decreases with time approaching asymptotically its quasi-steady state value. Note that the axial velocity inside the boundary layer increases at the early times and then decreases monotonically while the boundary-layer thickness is always decreasing, there will hence be a time when the flow rate in the boundary layer is maximum resulting in a more efficient heat-transfer mechanism. For this experiment the time is about 4 minutes. Miller [10] solved this problem for $Ra_L^* = 4 \times 10^9$ and showed how the heat-transfer mechanism is greatly improved during the early times. More experimental verification is necessary at low Ra_L^* for the complete transient problem.

Experimental error analysis

The main sources of error in this experiment are: the relative position of the probe volume with respect to the wall, the angle between the two laser beams, the finite size of the probe volume, the change of index of refraction with temperature, multiple particles at the probe volume, the local insulation effect of the reflective film, the estimation of the heat input, the frequency shift and the signal processor.

Many of these errors are very small compared to the total error and can be neglected. For instance, the signal processor was tested with a frequency generator and proved to be accurate. Multiple particles in the probe volume result in a signal with a varying phase and amplitude distribution. The signal processor utilized contains a signal verification system that virtually eliminates this problem for high particle concentration.

The reflective strip will reduce locally the heat flux to the fluid; however, the velocity at any point is a function of the conditions in the whole enclosure. To measure this effect, a second strip was placed on top of the first one and the conditions of a given experiment were reproduced. No measurable change in the velocity was observed. The finite size of the probe volume will result in a broad velocity distribution since particles moving inside the probe volume will have different velocities depending on the position where they cross the fringes. For an almost linear velocity profile inside the boundary layer there is an averaging effect when the velocity is

integrated for a short period of time. There will be some difficulty though in estimating the maximum velocity.

(a) The change in index of refraction would move the probe volume while heating the system. To minimize this error the maximum change in temperature was kept under 5°C between the time the probe volume was positioned and the end of the experiment. This change in index of refraction produces a change in the position of the probe volume of 0.06 mm.

(b) The maximum error in the position of the probe volume is ± 0.08 mm in the boundary layer. This error increases towards the center of the tank but the velocity is almost flat in this zone and no velocity change can be observed by moving the probe volume in the order of 1 mm. Combining (a) and (b) there is a total uncertainty of up to $+0.14$ mm, -0.08 mm in the position of the probe volume inside the boundary layer. The maximum velocity gradient across the boundary layer for $Ra_L^* = 6.4 \times 10^{10}$ is $dU/dR = 2\,s^{-1}$, hence the maximum error due to positioning the probe volume $2\,s^{-1} \times 0.14$ mm $= 0.28$ mm/s which is 10% of the maximum velocity.

(c) The angle between the two laser beams (θ) is known with an accuracy of 0.05° of a total of 12°. This yields to an absolute error in the frequency to velocity conversion (equation 4) of:

$$(100)\left[\frac{\sin(12.05/2)}{\sin(12/2)} - 1\right] = 0.4\%.$$

(d) The error in the frequency shift is ± 10 Hz which corresponds to an absolute error of ± 0.023 mm/s.

Combining all the sources of inaccuracies, a maximum error of $+12\%$, -8% can be expected in the velocity measurements. The difference between the ascending flow rate (inside the boundary layer) and the descending flow rate (core) was calculated to be less than 15% which is consistent with the total error. The error in the estimation of the boundary-layer thickness is due to the uncertainty in the position of the probe volume, that is $+0.14$ mm, -0.08 mm. The minimum value of δ_1 is 1.54 mm, which results in a maximum error of $+9\%$, -5%, which is consistent with the error observed in Fig. 11.

SUMMARY

The velocity profiles for a fluid contained in a cylinder subject to constant heat flux are presented for modified Rayleigh numbers of 4.5×10^9, 2.5×10^{10} and 6.4×10^{10}. It is shown that the flow field is different from that on a vertical flat plate due to the recirculating zone and the presence of the top. The flow field can be divided into three regions throughout the height of the tank. The radial dependance of the axial velocity is fit with a parabolic distribution in all three regions. The dependance of the axial velocity with the axial coordinate is different in each region. In Region I the velocity grows with $(h/L)^{3/5}$, in Region II it remains approximately constant and in Region III it changes linearly to zero on the top, indicating the presence of a boundary layer, due to the radial component of the velocity. Equations (5), (6) and (8) summarize this behavior.

The experimental results are compared with the numerical solution of Miller [10] and excellent agreement is observed as indicated in Figs. 6, 7, 8, 10 and 11.

Acknowledgement—This work was supported by the National Science Foundation, Grant ENG-77-12951.

REFERENCES

1. J. A. Clark, A review of pressurization, stratification and interfacial phenomena, *Adv. Cryogen. Engng* **8**, 259 (1964).
2. R. G. Schwind and G. C. Vliet, Observations and interpretations of natural convection and stratification in vessels, *Proc. Heat Transf. Fluid Mech. Inst.* **51**, 52 (1964).
3. B. D. Neff and C. W. Chiang, Free convection in a container of cryogenic fluid, *Adv. Cryogen. Engng* **12**, 117 (1966).
4. L. B. Evans, R. C. Reid and E. M. Drake, Transient natural convection in a vertical cylinder, *A.I.Ch.E. Jl* **14**(2), 251 (1968).
5. S. C. Fan and J. C. Chu, Thermal stratification in closed, cryogenic containers, *Adv. Cryogen. Engng* **14**, 249 (1968).
6. S. C. Huntley, Temperature–pressure–time relations in a closed cryogenic container, *Adv. Cryogen. Engng* **3**, 342 (1960).
7. E. Y. Harper, J. H. Chin, S. E. Hurd, A. M. Levy and H. M. Satterlee, Analytical and experimental study of liquid orientation and stratification in standard and reduced gravity fields, preliminary report, Lockheed Missile and Space Co. Contract NAS 8-11525, George C. Marshall Space Flight Center (1964).
8. L. B. Evans and N. R. Stefany, An experimental study of heat transfer to liquids in cylindrical enclosures, presented at the 8th National Heat Transfer Conference, Los Angeles, CA (1965).
9. J. Z. Barakat and J. A. Clark, Analytical and experimental study of the transient laminar natural convection flows in partially-filled liquid containers, in *International Heat Transfer Conference*, Vol. 2, p. 152 (1966).
10. C. W. Miller, Personal communication.
11. C. W. Miller, The effect of a thermally conducting wall on a stratified fluid in a cylinder, AIAA Paper No. 77-792, presented at the 12th Thermophysics Conference (1977).
12. M. C. Jischke and R. T. Doty, Linearized buoyant motion in a closed container, *J. Fluid Mech.* **71**, 729 (1975).
13. S. Ostrach, Natural convection in enclosures, *Adv. Heat Transfer* **8**, 161 (1972).
14. J. D. Trolinger, Laser instrumentation for flow field diagnostics, AGARDograph, No. 186 (1974).
15. F. Durst, *Principles and Practice of Laser-Doppler Anemometry*. Academic Press, New York (1976).

CONVECTION NATURELLE DANS UN CYLINDRE VERTICAL SOUMIS A UN FLUX THERMIQUE CONSTANT

Résumé—Une étude expérimentale utilise un vélocimètre laser Doppler pour mesurer la vitesse axiale d'un fluide contenu dans un cylindre soumis à un flux de chaleur uniforme sur la paroi latérale. On peut déceler des vitesses aussi faibles que 0,025 cm/s. L'erreur sur les vitesses typiques de couche limite est de $\pm 10\%$. Les nombres de Rayleigh modifiés varient entre $4{,}5 \times 10^9$ et $6{,}4 \times 10^{10}$ ce qui correspond à la limite supérieure du régime laminaire. Le champ de vitesse dans la couche limite est divisé en trois régions le long de l'axe du cylindre et une répartition parabolique est utilisée pour représenter les résultats dans chaque région. On trouve un excellent accord avec une solution numérique disponible.

FREIE KONVEKTION IN EINEM VERTIKALEN ZYLINDER BEI KONSTANTER WÄRMESTROMDICHTE

Zusammenfassung—Es wurde eine experimentelle Untersuchung durchgeführt, bei der mit einem Laser-Doppler-Anemometer die axiale Geschwindigkeit eines Fluids innerhalb eines Zylinders gemessen wurde, an dessen Seitenwänden eine konstante Wärmestromdichte vorlag. Dabei konnten so geringe Geschwindigkeiten wie 0,025 cm/s gemessen werden. Der Fehler bei typischen Geschwindigkeiten in der Grenzschicht beträgt $\pm 10\%$. Der untersuchte Bereich der modifizierten Rayleigh-Zahlen lag zwischen $4{,}5 \times 10^9$ und $6{,}4 \times 10^{10}$, was der oberen Grenze des laminaren Strömungsbereichs entspricht. Das Strömungsfeld innerhalb der Grenzschicht wurde in drei Gebiete in Längsrichtung des Zylinders unterteilt, und eine parabolische Verteilung wurde gewählt, um die Meßwerte innerhalb jedes Gebiets zu korrelieren. Eine sehr gute Übereinstmmmung mit einer vorhandenen numerischen Lösung wurde festgestellt.

ЕСТЕСТВЕННАЯ КОНВЕКЦИЯ В ВЕРТИКАЛЬНОМ ЦИЛИНДРЕ ПРИ ПОСТОЯННОМ ПОДВОДЕ ТЕПЛА

Аннотация — С помощью лазерного Допплеровского измерителя скорости проведены измерения аксиальной скорости жидкости в цилиндре при постоянном тепловом потоке на стенке. Прибор позволяет измерять минимальные значения скорости вплоть до 0,025 см/сек. Для типичных скоростей в пограничном слое ошибка составляла $\pm 10\%$. Исследуемые значения числа Релея изменялись в диапазоне $4{,}5 \times 10^9$–$6{,}4 \times 10^{10}$, что соответствовало верхнему пределу ламинарного режима. Поле потока в пределах пограничного слоя подразделялось на три области по оси цилиндра, и для обобщения данных в пределах каждой области использовалось параболическое распределение. Получено хорошее совпадение с имеющимся численным решением.